ORNL/TM-2017/12

# Compare optimized performance results for packaged RTU using all alternative refrigerants – FY17 1st Quarter Milestone Report


Bo Shen
Omar Abdelaziz
Som Shrestha
Ahmed Elatar
**12/31/2016**



OAK RIDGE NATIONAL LABORATORY
MANAGED BY UT-BATTELLE FOR THE US DEPARTMENT OF ENERGY

**ORNL/TM-2017/12**

# BTO Project 3.2.2.19
# FY17 1st Quarter Milestone Report

# Low-GWP Refrigerant Evaluation in AC Systems for High Ambient Temperature Applications - Compare optimized performance results for packaged RTU using all alternative refrigerants

**Authors**
**Bo Shen, Omar Abdelaziz, Som Shrestha, Ahmed Elatar**

**Date: 12/31/2016**

Prepared by
OAK RIDGE NATIONAL LABORATORY
Oak Ridge, TN 37831-6283
managed by
UT-BATTELLE, LLC
for the
US DEPARTMENT OF ENERGY
under contract DE-AC05-00OR22725

**Compare optimized performance results for packaged RTU using all alternative refrigerants (regular milestone)**

## Executive Summary

Based on laboratory investigations in FY16 for R-22 and R-410A alternative low GWP refrigerants in two baseline rooftop air conditioners (RTU), we used the DOE/ORNL Heat Pump Design Model to model the two RTUs and calibrated the models against the experimental data. Using the calibrated equipment models, we compared the compressor efficiencies and heat exchanger performances. An efficiency-based compressor mapping method was developed, which is able to predict compressor performances of the alternative low GWP refrigerants accurately.

Extensive model-based optimizations were conducted to provide a fair comparison between all the low GWP candidates by selecting their optimal configurations at the same cooling capacity and compressor efficiencies. The results illustrate that all the R-22 low GWP refrigerants will lead to slightly lower EERs. ARM-20B appears the best R-22 replacement due to its compatible EER and compressor displacement volume. However, at higher ambient temperatures, ARM-20A is the better candidate because its pressure ratio increases more slowly with the ambient temperature than the other refrigerants, which mitigates the degradation in the compressor efficiencies. In contrast, all R-410A low GWP candidates will result in similar or better efficiencies than R-410A. R-32 has the best EER and heat transfer performance while requiring the smallest compressor. However, R-32's pressure ratio increases the most with ambient temperature, which impairs its high ambient performance and may require more modifications on the compressor and system. R-452B appears to be the most suitable drop-in replacement, as it uses the closest compressor displacement volume and achieves the same efficiency as R-410A.

## Introduction

In FY16, the ORNL team evaluated a number of low GWP refrigerants as drop-in replacement for R-22 and R-410A in two baseline rooftop air conditioners (RTU): a 27.2 kWth (7.7 TR) R-22 system from SKM; PACL Series, model number PACL-51095Y (380/415V, 3 Phase, 50 Hz) and a 38.7 kWth (11 TR) R-410A system from Petra; PPH Series, model PPH4 115 (460V, 3 Phase, 60 Hz).

The alternative low GWP refrigerants for R-22 and R-410A are introduced in Tables 1 and 2, respectively, as below.

Table 1. Alternative Low GWP Replacements for R-22

| Refrigerant | GWP AR4 | GWP AR5 | Safety Class | Glide in Condenser [K] | Glide in Evaporator [K] | Critical Temperature [C] | Vendor |
|---|---|---|---|---|---|---|---|
| R-22 (baseline) | 1810 | 1760 | A1 | 0.0 | 0.0 | 96.16 | N/A |
| R-444B[a] | 295 | 295 | A2L | 7.6 | 8.9 | 92.11 | Honeywell |
| R-454A[b] (XL-40) | 239 | 238 | A2L | 5.4 | 6.2 | 78.94 | Chemours |
| ARM-20A[c] | 139 | 139 | A2L | 6.1 | 6.9 | 90.15 | Arkema |
| ARM-20B[d] | 251 | 251 | A2L | 5.3 | 6.0 | 88.74 | Arkema |

[a] R-444B has mass-based compositions of R-32 (0.415)/ R-1234ze(E) (0.485)/R-152a (0.1).
[b] R-454A (XL-40) has mass-based compositions of R-32 (0.35)/ R-1234yf (0.65).
[c.] ARM-20A has mass-based compositions of R-32 (0.18)/R-1234yf (0.7)/R-152a (0.12).
[d.] ARM-20B has mass-based compositions of R-32 (0.35)/R-1234yf (0.55)/R-152a (0.1).

Table 2. Alternative Low GWP Replacements for R-410A

| Refrigerant | GWP AR4 | GWP AR5 | Safety Class | Glide in Condenser [K] | Glide in Evaporator [K] | Critical Temperature [C] | Vendor |
|---|---|---|---|---|---|---|---|
| R-410A[a] (baseline) | 2088 | 1924 | A1 | 0.1 | 0.1 | 71.34 | N/A |
| R-32 | 675 | 677 | A2L | 0.0 | 0.0 | 78.12 | Daikin |
| R-452B[b] (DR-55) | 698 | 676 | A2L | 1.2 | 1.3 | 79.68 | Chemours |
| ARM-71A[c] | 460 | 461 | A2L | 1.8 | 2.1 | 81.52 | Arkema |
| R-447A[d] (L41-z) | 740 | 714 | A2L | 3.3 | 3.9 | 80.73 | Honeywell |

[a] R-410A has mass-based compositions of R-32 (0.5)/R-125 (0.5).
[b] .R-452B (DR-55) has mass-based compositions of R-32 (0.67)/R-125 (0.07)/R-1234yf (0.26).
[c] ARM-71A has mass-based compositions of R-32 (0.68)/R-1234yf (0.26)/ R-1234ze(E) (0.06).
[d] R-447A (L41-z) has mass-based compositions of R-32 (0.68)/R-125 (0.08)/R-1234ze(E) (0.24).

The two RTUs were tested in the ORNL commercial HVAC environmental chambers, strictly following the test conditions given in Table 3.

Table 3. Test Conditions

| Test condition | Outdoor[a] | Indoor | | | |
|---|---|---|---|---|---|
| | Dry-bulb temperature | Dry-bulb temperature | Wet-bulb temperature | Dew point temperature[b] | Relative humidity[b] |
| AHRI rated condition[b] | 35.0 (95) | 26.7 (80.0) | 19.4 (67) | 15.8 (60.4) | 50.9 |
| T3 | 46 (114.8) | 29 (84.2) | 19 (66.2) | 13.7 (56.6) | 39 |
| Hot | 52 (125.6) | 29 (84.2) | 19 (66.2) | 13.7 (56.6) | 39 |
| Extreme | 55 (131) | 29 (84.2) | 19 (66.2) | 13.7 (56.6) | 39 |

[a] There is no specification for the outdoor relative humidity as it has no impact on the performance.
[b] Per AHRI Standard 340/360.

## Thermodynamic properties of Low-GWP alternative refrigerants

The temperature-enthalpy diagram of a refrigerant illustrates two critical properties: the span between the saturated liquid line and saturated vapor line (i.e. latent heat of vaporization per unit mass of refrigerant) and the critical temperature (working range). Volumetric vaporization heat, i.e. latent heat × vapor density at an average saturation temperature of dew point and bubble point, indicates the evaporating capacity per volumetric flow rate. Refrigerants with smaller volumetric vaporization heat have reduced cooling capacities at the same average saturation temperature and compressor displacement volume.

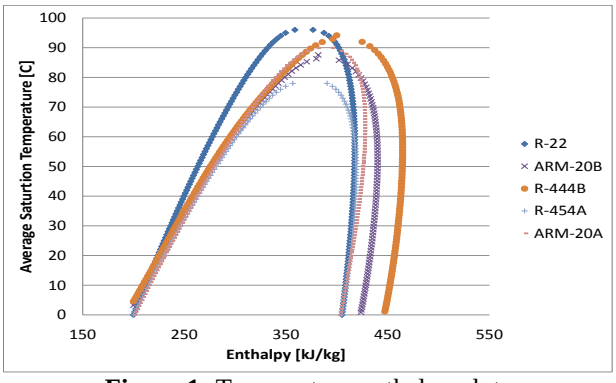


**Figure 1:** Temperature-enthalpy plots of R-22 alternatives

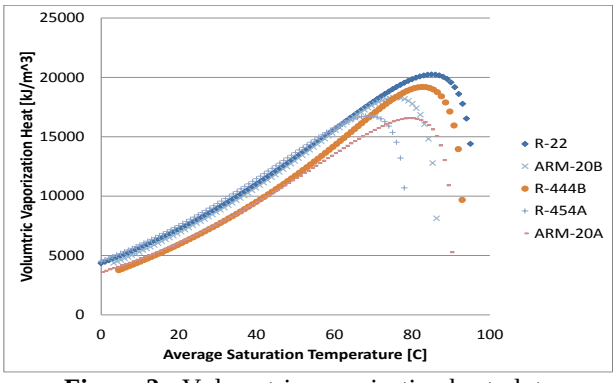


**Figure 2:** Volumetric vaporization heat plots of R-22 alternatives

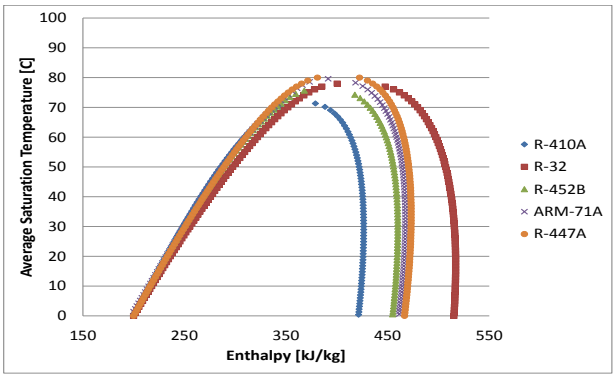


**Figure 3:** Temperature-enthalpy plot of R-410A alternatives

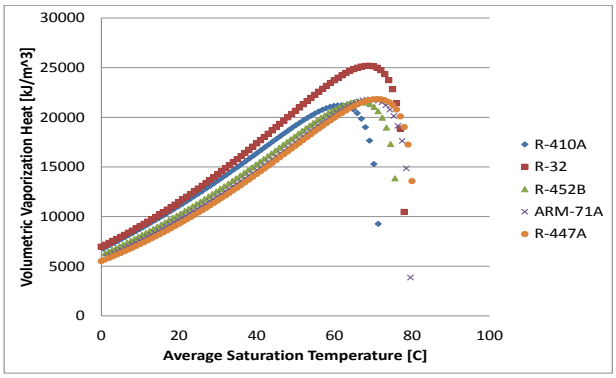


**Figure 4:** Volumetric vaporization heat plot of R-410A alternatives

Figure 1 illustrates the temperature-enthalpy diagram of the R-22 alternative refrigerants. All the R-22 alternatives have smaller working range, due to their lower critical temperatures. Figure 3 illustrates the temperature-enthalpy diagram of the R-410A alternative refrigerants. All the R-410A alternatives have wider domes and higher critical temperatures than R-410A, indicating that they are better refrigerants for high ambient operation. Figure 2 illustrates the volumetric vaporization heat versus the average saturation temperature for the R-22 alternatives. It shows that R-444B and ARM-20A have smaller volumetric vaporization heat. Figure 4 shows the volumetric vaporization heat versus the average saturation temperature for the R-410A alternatives. It illustrates that R-32 has the largest volumetric vaporization heat and R-410A is second.

Figure 5 shows curves of saturation temperature versus density of the R-22 alternatives. It can be seen that the alternative refrigerants have smaller vapor density than R-22, which indicates that the low GWP refrigerants will have smaller refrigerant mass flow rate using the baseline R-22 compressor and result in smaller coil refrigerant pressure drops. Figure 6 shows these properties for the R-410A alternatives. The R-410A alternatives will also lead to reduced refrigerant mass flow rates, but to a lesser degree.

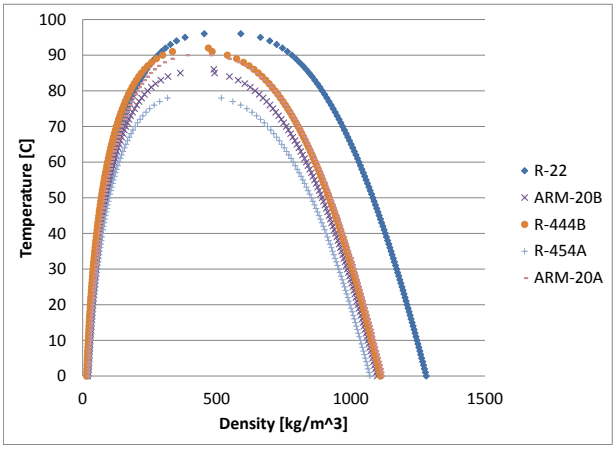


**Figure 5:** Saturation temperature-density curves of R-22 alternatives

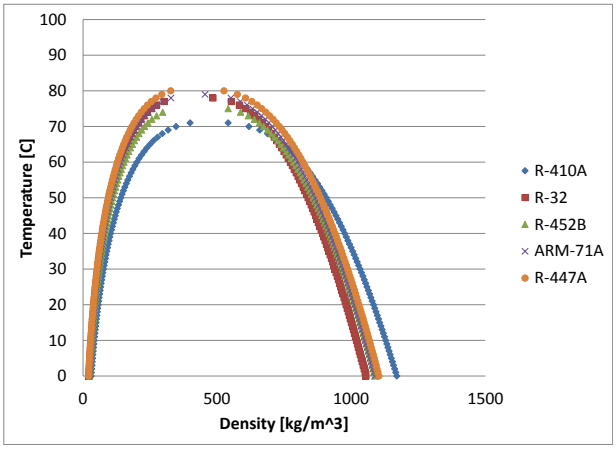


**Figure 6:** Saturation temperature-density curves of R-410A alternatives

At the same average saturation temperature, a refrigerant with a lower volumetric vaporization heat results in smaller cooling capacity during a drop-in replacement. On the other hand, the saturation temperature is impacted by the heat transfer performance and refrigerant pressure drop of the refrigerant. Lower saturation temperature leads to smaller cooling capacity if using the same compressor. And thus,

whether an alternative low GWP refrigerant will lead to higher or lower capacity depends on the trade-off between its volumetric vaporization heat and the resultant suction saturation temperature.

## Model Calibration

We used the DOE/ORNL Heat Pump Design Model (HPDM) to model the two baseline RTUs, and calibrated the RTU system and component models against the lab data for each refrigerant. The most current version of the HPDM (Flex-HPDM) has a flexible solver such that any variables can be given or solved. That means users can switch between knowns and unknowns in the system solving. For the model calibrations, we input the measured refrigerant mass flow rate, compressor power, pressures, and temperatures as known variables and then solved for the compressor efficiencies and the two-phase heat transfer coefficients in the condenser and evaporator as unknowns. A two-step solving procedure was applied to decouple the refrigerant-side and air-side heat transfer. Because HPDM's refrigerant-side heat transfer correlations for R-22 and R-410A have been well developed and documented in the literature, the refrigerant side heat transfer calculations are considered accurate for the R-22 and R-410A data. For the first step, we reduced the air side heat transfer coefficient for the R-22 and R-410A baseline units using the original refrigerant side heat transfer correlations. As the RTUs have constant indoor and outdoor air flow rates, the air side heat transfer should not change when operating with other alternative refrigerants. For the second step, we treated the calculated air side heat transfer coefficients as knowns, and calculated the refrigerant side two-phase heat transfer coefficients specific to each alternative refrigerant. Further, the phase allocation ratios, i.e. single-phase versus two-phase, are predicted by the HPDM model.

Figure 7 shows the calculated volumetric efficiencies as a function of the compressor pressure ratio (discharge pressure/suction pressure) for the R-22 alternative refrigerants, when changing the ambient temperature from 95°F to 125°F. Figure 8 shows the isentropic efficiencies. A general trend is observed that the compressor efficiencies decrease with the pressure ratio. It can be seen that R-444B, ARM-20B and R-454A have a similar range of pressure ratios as R-22, from 95°F to 125°F ambient temperature. However, ARM-20A's pressure ratio increases more slowly with increasing ambient. Consequently, ARM20A has better efficiencies at high ambient temperatures, i.e. 115°F and 125°F.

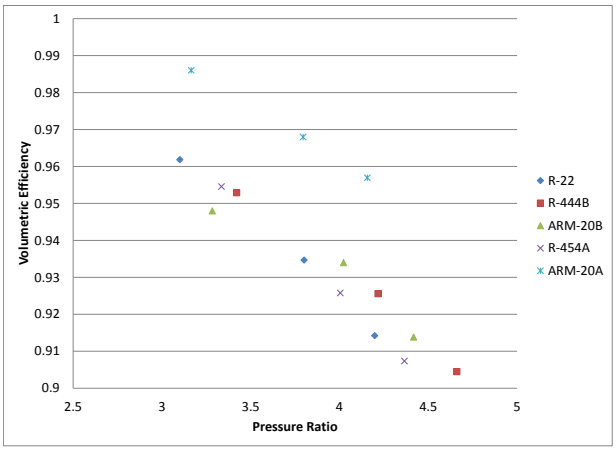


**Figure 7:** Compressor volumetric efficiencies of R-22 alternatives

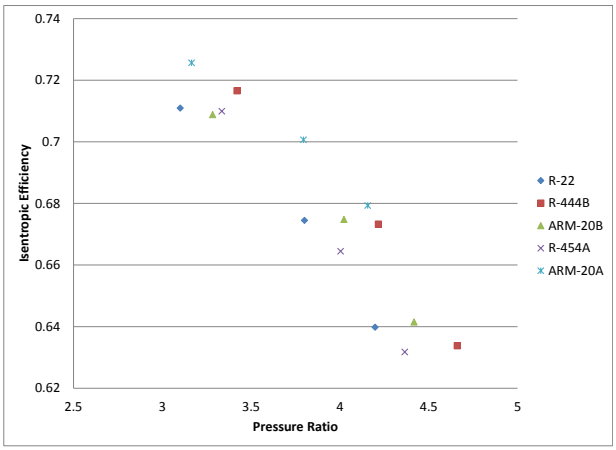


**Figure 8:** Compressor isentropic efficiencies of R-22 alternatives

Figure 9 shows the calculated volumetric efficiencies of the R-410A alternative refrigerants for ambient temperatures ranging from 95°F to 131°F. Figure 10 shows the isentropic efficiencies. Except for R-32, the other low GWP refrigerants have a similar range of pressure ratios and compressor efficiencies as R-410A. R-32 has higher pressure ratios than the other refrigerants, especially at the high ambient

temperatures of 125°F and 131°F, which leads to noticeably lower compressor efficiencies. This indicates that the compressor should be re-designed if applying R-32.

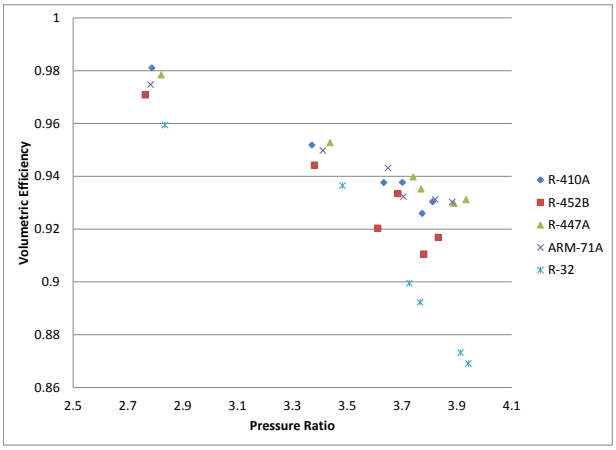


**Figure 9:** Compressor volumetric efficiencies of R-410A alternatives

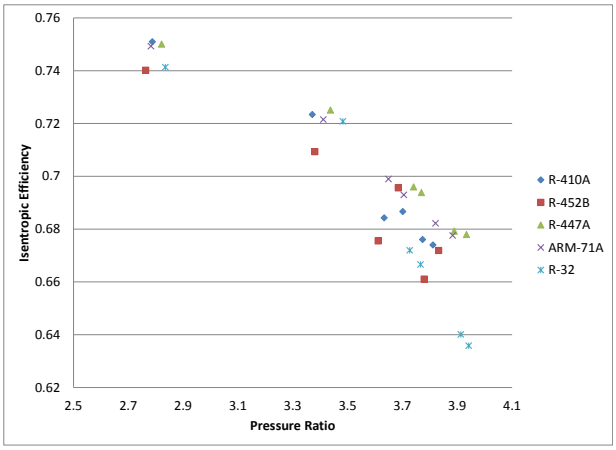


**Figure 10:** Compressor isentropic efficiencies of R-410A alternatives

We compared overall heat transfer coefficients in the two-phase region of the condenser and evaporator of the alternative refrigerants, relative to their baseline refrigerants, with the original heat exchanger designs. The two-phase overall heat transfer coefficient includes both air-side and refrigerant-side heat transfer, measured at 95°F ambient temperature. Figure 11 compares the R-22 alternative refrigerants, and Figure 12 compares R-410A alternatives. R-32 resulted in better overall heat transfer in both the condenser and evaporator. However, all the other alternatives led to slightly poorer heat transfer performance.

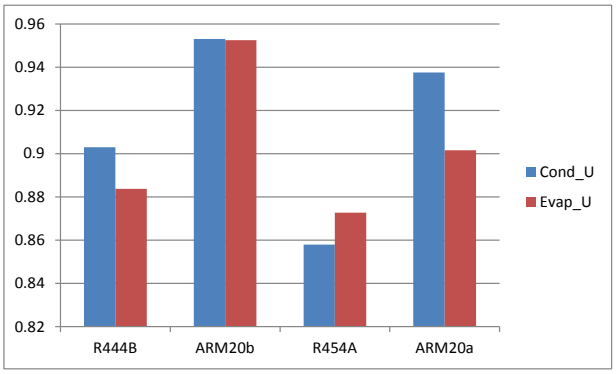


**Figure 11:** Overall two-phase heat transfer coefficients, relative to R-22

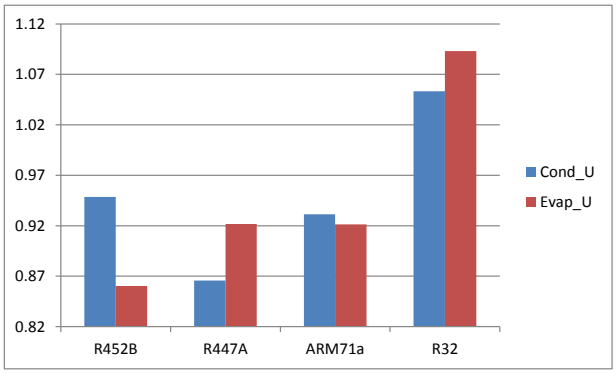


**Figure 12:** Overall two-phase heat transfer coefficients, relative to R-410A

## Compressor Performance Mapping Method for Drop-in Replacements using Alternative Low GWP Refrigerants

AHRI 10-coefficient compressor maps (ANSI/AHRI 540-99, 2010) are used to calculate mass flow rate and power consumption, and the calculation of the refrigerant-side versus air-side energy balance from inlet to outlet is enabled by the additional input of a compressor shell loss ratio relative to the power input. We also consider the actual suction state to correct the map mass flow prediction using the method of Dabiri and Rice (1981).

Manufacturers usually developed their 10-coefficient compressors specific to individual refrigerants. We need to develop a compressor mapping method for drop-in replacements using low GWP alternatives. For this study, we obtained the original compressor maps, i.e. Copeland scroll ZR108KC-TFD developed for R-22 and ZP120KCE-TFD developed for R-410A. For modeling alternative refrigerants, it is assumed that the compressor would maintain the same volumetric and isentropic efficiencies at the same suction and discharge pressures. Thus, the efficiencies were reduced from the original map as a function of the suction and discharge pressures. The volumetric efficiency and isentropic efficiency are used in evaluating the compressor performance as shown in Equations 1 and 2 respectively.

$$m_r = Volume_{displacement} \times Speed_{rotation} \times Density_{suction} \times \eta_{vol} \quad (1)$$

$$Power = m_r \times (H_{discharge,s} - H_{suction})/\eta_{isentropic} \quad (2)$$

Where $m_r$ is the compressor mass flow rate; $Power$ is compressor power; $\eta_{vol}$ is compressor volumetric efficiency; $\eta_{isentropic}$ is compressor isentropic efficiency; $H_{suction}$ is compressor suction enthalpy; $H_{discharge,s}$ is the enthalpy obtained at the compressor discharge pressure and suction entropy.

Table 4 presents max and standard deviations using the mapping method to predict refrigerant mass flow rates ($m_r$) and compressor power (*Power*), in comparison to the measured values for each refrigerant, as the ambients ranged in temperature from 95°F to 131°F. It can be seen that the converted, efficiency-based compressor map can be used for the alternative refrigerants, and the predictions reach the same level of accuracy as for the baseline refrigerant, i.e. R-22 or R-410A, for which the compressor map was developed. The largest prediction error of 7.0% is related to predicting the R-32 mass flow rate at 131°F ambient temperature, where the compressor efficiency degrades drastically at the high pressure ratio.

Table 4. Deviations in predicting compressor mass flow rate and power

| | **R-22** | **R-444B** | **R-454A** | **ARM-20A** | **ARM-20B** |
|---|---|---|---|---|---|
| Max Deviation, Mr | 3.1% | 2.6% | 1.7% | 2.7% | 1.1% |
| Standard Dev, Mr | 0.5% | 0.3% | 1.3% | 1.3% | 1.1% |
| Max Deviation, Power | 4.5% | 2.5% | 3.4% | 4.8% | 3.0% |
| Standard Dev, Power | 0.1% | 1.4% | 1.5% | 0.6% | 1.5% |
| | **R-410A** | **R-452B** | **ARM-71A** | **R-447A** | **R-32** |
| Max Deviation, Mr | 1.1% | 3.9% | 2.8% | 4.2% | 7.0% |
| Standard Dev, Mr | 0.5% | 0.8% | 0.5% | 0.8% | 1.9% |
| Max Deviation, Power | 4.4% | 3.9% | 2.9% | 3.2% | 2.6% |
| Standard Dev, Power | 0.3% | 0.5% | 0.2% | 0.3% | 0.9% |

The above analysis indicates that this approach can be employed with reasonable accuracy to represent the performance of existing compressors when used with low-GWP alternatives, in lieu of actual compressor test data with such alternatives. While this mapping was not used in the single-point optimizations which follow, it provides a path forward to predict the IEERs of RTU's based on calibrated system models from our laboratory RTU testing with the eight low-GWP alternatives.

**System Optimizations**

The drop-in investigation doesn't provide a fair comparison between all the refrigerants, because the RTUs were originally designed for R-22 and R-410A. The alternative refrigerants led to different cooling capacities, which caused the heat exchangers to be somewhat unloaded or overloaded, compared to the original design. Some alternative refrigerants have large temperature glides, and they would prefer different heat exchanger configurations. In addition, being different from the drop-in replacement using the compressor developed for a baseline refrigerant, the compressor design should be optimized for each individual refrigerant once a refrigerant is launched to the market in a big scale. We expect that one

alternative low GWP refrigerant will at least reach the same compressor efficiency level as its baseline refrigerant.

Considering the above we conducted a model-based system optimization of unit EER at AHRI rating conditions. We assumed a constant compressor isentropic efficiency and volumetric efficiency at design ambient conditions, based on the measured values from testing the baseline refrigerant (R-22 alternatives: volumetric efficiency = 96%, isentropic efficiency = 71%; R-410A alternatives: volumetric efficiency = 99%; isentropic efficiency = 75%); however, we allowed the compressor displacement volume to vary in order to match the target capacity (R-22 alternatives: 7.7 TR; R-410A alternatives: 11 TR). The compressor suction superheat degree was recommended by Honeywell for each refrigerant (baseline superheat – 0.8 * temperature glide at the suction pressure/2.0). The condenser exit subcooling degree, i.e., a surrogate for the refrigerant system charge, was optimized along with the heat exchanger circuitry to maximize efficiency at a fixed design capacity. To provide a fair comparison at the same cooling capacity by locating the optimized heat exchanger configuration of each refrigerant in a large population, we conducted a series of optimization studies as per the following matrix:

- Three heat exchanger flow directions (green cells represent tubes), respectively for condenser and evaporator

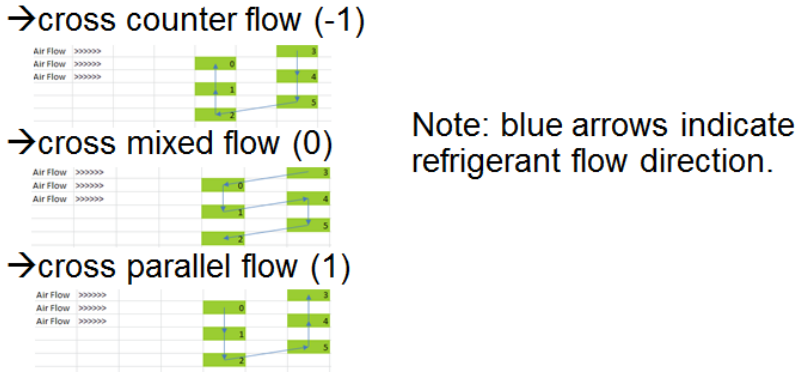


**Figure 13:** Heat exchanger flow patterns

- Varying evaporator circuit numbers: R-22 alternatives – 6, 8, 12 (distribute 72 tubes evenly among the circuits in three rows); R-410A alternatives – 8, 12, 24 (distribute 144 tubes evenly among the circuits in six rows)
- Varying condenser circuit numbers: R-22 alternatives – 4, 6, 8 (distribute 96 tubes evenly among the circuits in two rows); R-410A alternatives – 8, 12, 16 (distribute 192 tubes evenly among the circuits in four rows)

Therefore, the population of each refrigerant at one capacity, contains 3 (evaporator flow patterns) ×3 (condenser flow patterns) × 3 (evaporator circuit numbers) × 3 (condenser circuit numbers) = 81 cases. It should be mentioned that we kept the same indoor and outdoor fan air flow rates and power consumption, tube sizes, and calibrated air side and refrigerant side heat transfer using the experimental data. In all simulations, we kept the same heat exchanger sizes and fan performances. Throughout the heat exchanger design optimization, both the circuitry and the condenser subcooling were varied to obtain maximum design point efficiency while adjusting the compressor displacement individually for the 81 cases to maintain design capacity.

Figure 14 shows the optimized EERs and compressor volumes of the R-22 alternatives relative to the R-22 optimized case. Figure 15 shows the optimized EERs and compressor volumes of the R-410A alternatives. Table 5 lists the corresponding parameters leading to the optimized results. When providing the same capacity, all the R-22 alternatives result in slightly lower EERs than R-22. R-444B and ARM-

20A require larger compressors, and ARM-20B and R-454A need smaller compressors. All the R-410A alternatives reach similar or better EERs and R-32 has the highest efficiency. R-452B requires a similar compressor volume and R-32 requires a smaller compressor. R-447A and ARM-71A need somewhat larger compressors to deliver the same capacity.

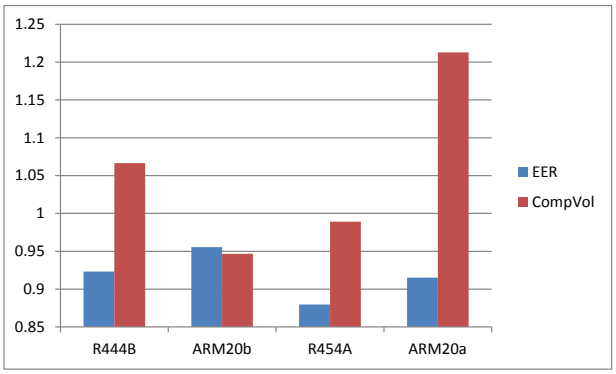


**Figure 14:** Optimized EERs and compressor displacement volumes of R-22 alternatives

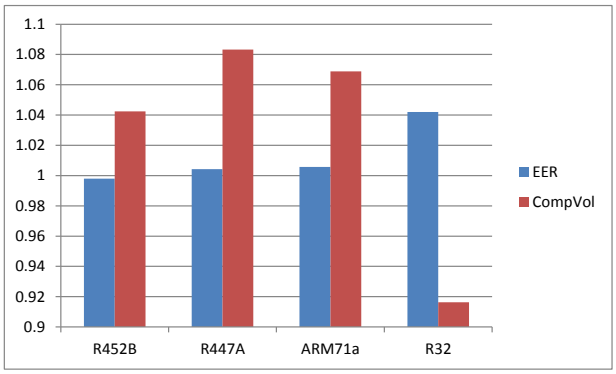


**Figure 15:** Optimized EERs and compressor displacement volumes of R-410A alternatives

Table 5. Optimized parameters

| | **R-22** | **R-444B** | **R-454A** | **ARM-20A** | **ARM-20B** |
|---|---|---|---|---|---|
| Condenser flow pattern | Counter | Counter | Counter | Counter | Counter |
| Evaporator flow pattern | Mixed | Counter | Counter | Counter | Counter |
| Condenser circuit number | 8 | 8 | 6 | 8 | 8 |
| Evaporator circuit number | 12 | 12 | 12 | 12 | 12 |
| Condenser subcooling [R] | 13.8 | 10.4 | 12.5 | 11.0 | 11.5 |
| Evaporator superheat [R] | 12.0 | 6.0 | 7.5 | 7.0 | 7.5 |
| | **R-410A** | **R-452B** | **ARM-71A** | **R-447A** | **R-32** |
| Condenser flow pattern | Counter | Counter | Counter | Counter | Counter |
| Evaporator flow pattern | Counter | Counter | Counter | Counter | Counter |
| Condenser circuit number | 8 | 8 | 12 | 8 | 8 |
| Evaporator circuit number | 24 | 24 | 24 | 24 | 24 |
| Condenser subcooling [R] | 17.8 | 16.3 | 14.5 | 15.5 | 15.0 |
| Evaporator superheat [R] | 12.0 | 11.0 | 10.5 | 8.5 | 12.0 |

## Conclusions

When matching the same cooling capacity and assuming the same compressor efficiencies at 95°F ambient, all R-22 low GWP refrigerants will lead to slightly lower EERs for RTU application. ARM-20B appears the best replacement due to its compatible EER and compressor displacement volume. However, at higher ambient temperatures, ARM-20A is the best candidate because its pressure ratio increases more slowly with the ambient temperature, which mitigates the degradation in the compressor efficiencies.

All R-410A low GWP candidates will result in similar or better efficiencies than R-410A. R-32 has the best efficiency, heat transfer performance, and requires the smallest compressor. However, R-32's pressure ratio increases most drastically with the ambient temperature, which impairs its high ambient performance and may require more modifications on the compressor and system. R-452B appears the most suitable drop-in replacement, as it uses a similar compressor displacement volume and achieves the same efficiency as R-410A for application to RTUs.

## References


Abdelaziz, O.A, Shrestha, S, Shen, B., Elatar, A., Linkous, R., Goetzler, W, Guernsey, M., Bargash, Y., 2016, *Alternative Refrigerant Evaluation for High-Ambient-Temperature Environments: R-22 and R-410A Alternatives for Rooftop Air Conditioners*, ORNL/TM-2016/513, available online at: http://info.ornl.gov/sites/publications/Files/Pub69980.pdf

*ANSI/AHRI Standard 540-99*, *2010, Positive Displacement Refrigerant Compressors and Compressor Units,* Air-Conditioning and Refrigeration Institute, Arlington, VA

Dabiri, A. E. and C.K. Rice, 1981. "A Compressor Simulation Model with Corrections for the Level of Suction Gas Superheat," *ASHRAE Transactions,* Vol. 87, Part 2, pp.771-782.

*AHRI Standard 340/360*, *2015, Performance Rating of Commercial and Industrial Unitary Air-conditioning and Heat Pump Equipment,* Air-Conditioning and Refrigeration Institute, Arlington, VA